Identification of SARS-CoV-2 in different human tissues. Validation of immunohistochemical and qPCR techniques in paraffin-embedded tissues and cytology

Irene Bernal-Florindo (iriberni@hotmail.com)
Biomedical Research and Innovation Institute of Cadiz
Antonio Santisteban-Espejo
Puerta del Mar University Hospital
Juan Del Rio-Ignacio
Jerez de la Frontera University Hospital
Pedro Muriel-Cueto
Puerta del Mar University Hospital
Jose Perez-Requena
Puerta del Mar University Hospital
Lidia Atienza-Cuevas
Puerta del Mar University Hospital
Inmaculada Catalina-Fernandez
Puerta del Mar University Hospital
Marcial Garcia-Rojo
Puerta del Mar University Hospital
Raquel Romero-Garcia
Biomedical Research and Innovation Institute of Cadiz

Article

Keywords:

Posted Date: March 24th, 2022

DOI: https://doi.org/10.21203/rs.3.rs-1441884/v1

Abstract

Since the beginning of 2020, severe acute respiratory syndrome coronavirus 2 (SARS-CoV-2) has been responsible for a global pandemic. Although the scientific community has focused on its study, there is little knowledge on validated techniques for detecting SARS-CoV-2 in formalin-fixed paraffin embedded (FFPE) tissues archived in pathology departments. The objective of this study was to validate immunohistochemistry (IHC) and quantitative polymerase chain reaction (qPCR) for the diagnosis of respiratory coronavirus disease 2019 (COVID-19) in cytology and FFPE tissues, obtained from multiple specimen types (autopsy, incisional biopsy and surgical specimens). We also defined relevant temporary points (interval, persistence and archival times) to evaluate the correlation between those periods and viral load. A total of 43 cytology and FFPE samples from patients with a previous positive qPCR COVID-19 test in nasopharyngeal swabs were analysed. Two different qPCR techniques were evaluated from IDT Technologies (method A) and Roche Diagnostics (method B). In immunohistochemistry, antibodies directed against nucleocapsid and spike viral proteins were employed. A total of 25.58% of the evaluated samples were positive for any of the two qPCR techniques. Only one placental specimen (3.44%) with acute villitis showed strong IHC positivity for both antibodies, and the other 4 specimens (lung, brain, kidney and placenta) showed isolated weakly positive cells with IHC. A strong statistically significant correlation was observed between threshold values for qPCR method A and interval time ($p = 0.01$; $\rho = 0.917$) and persistence time ($p = 0.002$; $\rho = 0.879$) and between qPCR method B and archival time ($p = 0.037$; $\rho = 0.900$). In conclusion, the qPCR technique is a sensitive diagnostic tool for SARS-COV-2 detection for both cytology and FFPE specimens. With currently available antibodies, IHC to detect the presence of SARS-COV-2 should only be used in special cases.

Introduction

Severe acute respiratory syndrome coronavirus 2 (SARS-CoV-2) is a new type of coronavirus that causes the respiratory coronavirus disease 2019 (COVID-19). This virus is responsible for the pandemic that emerged in Wuhan (China) at the end of 2019 due to its high infectivity and virulence capacity. COVID-19 is an encapsulated virus that contains single-stranded RNA as genetic material[1].

In clinical practice, the main validated diagnostic tests for COVID-19 are based on quantitative polymerase chain reaction (qPCR) techniques on specimens obtained using nasopharyngeal swabs, although the detection of antibodies in serology also has an important role in the clinical follow-up of this infection.

Different studies and investigations about the presence of SARS-CoV-2 in human tissues have been performed since the beginning of the pandemic. However, further research is necessary to confirm the best techniques to identify SARS-CoV-2 in special conditions, such as formalin-fixed paraffin-embedded (FFPE) tissues.

In this context, the limited number of histopathological studies on SARS-CoV-2 indicate that the main diagnostic findings are detected in respiratory, cardiovascular, digestive and neurological systems[2.3.4]. Although the main clinical manifestations of COVID-19 are respiratory, the involvement of other organs during the course of the infection is still under investigation[4].

In the case of the Middle East Respiratory Syndrome (MERS) of 2012, the presence of the virus could be studied by immunohistochemistry (IHC)[4], a technique poorly described in COVID-19. Some authors have validated the use of two antibodies for use in brightfield immunohistochemical techniques. One is a rabbit polyclonal antibody directed against the S glycoprotein (spike) that the virus uses to anchor itself to angiotensin-converting enzyme 2 (ACE2) in host cells. The other antibody corresponds to a mouse monoclonal antibody directed against the nuclear protein (NP) of the nucleocapsid of the virus.

Direct immunofluorescence and in situ hybridization techniques have also been developed that can be used in paraffin tissues and have helped to detect intracytoplasmic SARS-CoV-2 viral inclusions in type II pneumocytes and macrophages[5]. The first description of the use of qPCR techniques to detect SARS-CoV-2 virus in FFPE specimens was performed in 2020 in surgical samples of tongue squamous cell carcinoma[6].

The main aim of this study was to validate brightfield immunohistochemical and qPCR techniques to detect SARS-CoV-2 in cytology and in different FFPE human tissues.

Results

Samples from patients and interval, persistence and archival times

Table 1 shows the specimen type, main diagnosis, time periods and qPCR results of all the samples included in the study. The most frequent specimens were small biopsies (34.88%), followed by surgical specimens (27.91%) and liquid cytology samples (27.91%). Autopsies (6.98%) and cytology blocks (2.33%) were less frequent samples. The kidney (13.96%), placenta (11.63%), lung (6.35%) and oesophagus (6.35%) were the most frequent sample origins.

Table 1

List of samples and their origin, main diagnosis, time periods and qPCR results.

ID	Specimen type	Sample origin	Diagnosis	Interval	Persistence	Archival	qPCR result IDT Technologies (Cp)	qPCR result Roche Diagnostics (Cp)
1	Biopsy	Bladder	Urothelial carcinoma	72	20	240	Negative	Negative
2	Biopsy	Bone marrow	Normal (patient with leg lymphoma)	56	32	153	Negative	Not performed
3	Biopsy	Oesophagus	Severe intraepithelial neoplasia	59	17	168	Positive (38.74)	Negative
4	Biopsy	Oesophagus	Adenocarcinoma	73	17	154	Negative	Negative
5	Biopsy	Kidney	Transplantation; acute tubular necrosis	17	7	223	Positive (34.5)	Positive (36.9)
6	Biopsy	Kidney	Transplantation; no relevant alterations	34	67	238	Negative	Negative
7	Biopsy	Kidney	Active antibody-mediated transplant rejection	-52	102	101	Negative	Negative
8	Biopsy	Kidney	Transplantation; no relevant alterations	35	21	224	Negative	Negative
9	Biopsy	Kidney	Active antibody-mediated transplant rejection	-42	102	91	Negative	Negative
10	Biopsy	Large intestine	Normal (patient with diarrhoea)	29	10	114	Negative	Negative
11	Biopsy	Large intestine	Signet ring cell adenocarcinoma	75	71	140	Negative	Positive (35.8)
12	Biopsy	Liver	Hepatocarcinoma	31	27	111	Negative	Not performed
13	Biopsy	Nasal cavity	Esthesioneuroblastoma	1	17	196	Negative	Negative
14	Biopsy	Prostate	Adenocarcinoma	-47	39	202	Negative	Negative
15	Biopsy	Stomach	Active chronic gastritis	-16	6	134	Negative	Negative
16	Surgical	Brain	Glioblastoma	23	37	168	Negative	Negative
17	Surgical	Oesophagus	Distal oesophageal adenocarcinoma	95	9	331	Negative	Negative
18	Surgical	Lung	Intra-alveolar haemorrhage	2	13	294	Negative	Negative
19	Surgical	Lung	Amyloidosis	27	NA*	NA*	Negative	Negative
20	Surgical	Placenta	No relevant alterations	8	16	125	Negative	Negative
21	Surgical	Placenta	No relevant alterations	0	1	400	Negative	Negative
22	Surgical	Placenta	Acute villitis	0	1	122	Positive (14.55)	Positive (17.2)
23	Surgical	Placenta	No relevant alterations	1	3	150	Positive (9.14)	Negative
24	Surgical	Placenta	No relevant alterations	9	12	183	Positive (32.12)	Positive (28.09)
25	Surgical	Thyroid	Papillary carcinoma	-90	13	379	Negative	Negative
26	Surgical	Thyroid	Papillary carcinoma	30	13	259	Negative	Negative
27	Surgical	Ureter	Necrosis and acute	-45	21	304	Negative	Negative

			inflammation					
28	Autopsy	Lung	Interstitial pneumonitis	14	14	387	Positive (35.19)	Negative
29	Autopsy	Kidney	Inflammatory infiltrate	14	14	387	Negative	Negative
30	Autopsy	Brain	Infarcts	14	14	387	Negative	Positive (37.7)
31	Cytology block	Hepatic hilum lymph node	Oesophageal adenocarcinoma metastasis	-53	9	479	Negative	Not performed
32	Cytology	Ascitic fluid	Negative for malignancy	91	72	197	Positive (35.5)	Negative
33	Cytology	Bronchial aspirate	Negative (patient with leukaemia)	42	49	196	Negative	Not performed
34	Cytology	Bronchial aspirate	Negative for malignancy	25	NA*	139	Negative	Not performed
35	Cytology	Bronchoalveolar lavage	Negative for malignancy	25	NA*	139	Negative	Not performed
36	Cytology	Bronchoalveolar lavage	Negative (patient with leukaemia)	42	49	196	Negative	Negative
37	Cytology	Bronchoalveolar lavage	Negative for malignancy	41	36	416	Negative	Negative
38	Cytology	Cervix	Negative for HPV	353	37	104	Negative	Negative
39	Cytology	Oesophagus	Negative for malignancy	299	9	127	Negative	Negative
40	Cytology	Liver	Carcinoma	31	27	111	Negative	Negative
41	Cytology	Pleural fluid	Negative for malignancy	3	24	413	Negative	Not performed
42	Cytology	Pleural fluid	Negative inflammatory fluid	2	13	294	Positive (34.4)	Not performed
43	Cytology	Urine	Negative for malignancy	170	NA*	142	Positive (35.65)	Not performed

***NA** indicates that positive nasopharyngeal qPCR was not confirmed. Cp = qPCR crossing point

The mean interval time between nasopharyngeal qPCR positivity and pathology sample collection was 34.84 days (SD: 79.50 days; 95% CI: 10.37-59.30 days), the mean SARS-CoV-2 persistence time was 28.70 days (SD: 24.84 days; 95% CI: 21.05-36.34 days), and the mean archival time of the pathology sample was 220.88 days (SD: 107.00 days; 95% CI: 187.95-253.81 days). The different time periods defined did not follow a normal distribution ($p<0.001$).

Nucleic acid extraction and SARS-CoV-2 detection by qPCR

Cohen´s kappa index (κ) was 0.396 for the concordance between qPCR methods A and B. When compared, no statistically significant differences were observed between the results of both qPCR techniques ($p=0.063$, $\chi2 = 5.513$). Using qPCR from IDT Technologies, method A, a total of 9 (20.93%) samples tested positive for SARS-CoV-2. Specimens included both FFPE tissues (kidney, oesophagus, placenta and lung) and cytology samples (ascitic fluid, pleural fluid and urine). For qPCR from Roche Diagnostics, method B, the presence of SARS-CoV-2 was detected in a total of 5 (14.71%) samples, all of which corresponded to biopsies (kidney, large intestine, placenta and brain).

Immunohistochemical study

Only a syncytiotrophoblast specimen (case 22) showed strong diffuse IHC positivity for both the NP and spike proteins of SARS-CoV-2 (**Figure 1**). The lowest Cp values from qPCR method A (14.55) and qPCR method B (17.20) corresponded to this sample.

Positive staining was found in pneumocytes (sample 28), microglia in a patient with a clinical history of brain infarct (sample 30), isolated tubular epithelial cells of the kidney (sample 5) and inflammatory cells in the villi of a placenta without other relevant histopathological changes (sample 23) (**Figure 2**). All five IHC-positive samples also showed positivity using some of the two qPCR methods. The distribution by anatomical location and organ of the qPCR and IHC results for all cases studied is described in **Table 2**.

Table 2

Distribution of the qPCR and immunohistochemical results by organ and anatomical site for all samples studied

ORGAN (n)	qPCR POSITIVE (n)	IHC POSITIVE (n)
Upper respiratory system		
Nasal cavity (1)	0% (0/1)	0% (0/1)
Lower respiratory system		
Bronchial aspirate or Bronchoalveolar lavage (5)	0% (0/5)	Not performed
Lung (3)	33% (1/3)	33% (1/3)
Pleural fluid (2)	50% (1/2)	Not performed
Digestive system		
Oesophagus (4)	25% (1/4)	0% (0/3)
Large intestine (2)	50% (1/2)	0% (0/2)
Liver (2)	0% (0/2)	Not performed
Ascitic fluid (1)	100% (1/1)	Not performed
Genitourinary system and placenta		
Bladder or urine (2)	50% (1/2)	0% (0/1)
Kidney (6)	17% (1/6)	20% (1/5)
Prostate (1)	0% (0/1)	0% (0/1)
Placenta (5)	60% (3/5)	60% (3/5)
Ureter (1)	0% (0/1)	0% (0/1)
Cervix cytology (1)	0% (0/1)	Not performed
Urine (1)	100% (1/1)	Not performed
Central nervous system		
Brain (1)	100% (1/1)	100% (1/1)
Endocrine system		
Thyroid (2)	0% (0)	0% (0)
Haematolymphoid system		
Bone marrow (1)	0% (0/1)	0% (0/1)
Lymph node (1)	0% (0/1)	Not performed

Correlation between qPCR results and the periods of time (interval, persistence and archival)

To assess whether the viral load of SARS-CoV-2 in the samples studied was associated with variations in the time periods, we performed a correlation analysis. A statistically significant correlation was obtained for the association between the threshold values for qPCR method A and interval time (p=0.01) and SARS-CoV-2 persistence time (p=0.002) and for the association between the threshold values for qPCR method B and archival time (p=0.037).

Furthermore, correlation coefficients showed a strong correlation between qPCR method A and interval time (ρ=0.917), qPCR method A and persistence time (ρ=0.879), and qPCR method B and archival time (ρ=0.900). **Table 3** shows the results of the correlation analysis for all samples included in the study.

Table 3

Spearman correlation results between threshold values for both qPCR methods and periods of time. *Italicized values mean $p<0$.

	Threshold values for qPCR*	
Period of time	Method A (IDT Technologies)	Method B (Roche Diagnostics)
Interval time	*0.917*	0.600
Persistence time	*0.879*	0.500
Archival time	0.606	*0.900*

Discussion

This study demonstrated that it is possible to detect SARS-CoV-2 in several FFPE tissues and cytology specimens, mainly with qPCR techniques. While IHC was only useful in placental tissue with acute inflammation, qPCR also showed a high viral load. In this regard, qPCR techniques were more sensitive than IHC, with qPCR method A showing the highest percentage of positive cases (20.93%) and IHC using the spike primary antibody showing only 10.34% positivity.

The better sensitivity of qPCR method A may be due to both a better nucleic acid extraction method and a better qPCR process; its extraction process was fully automatic, and the qPCR method B extraction process was manual. Furthermore, method A was based on primers and probes from IDT technologies designed to detect the SARS-CoV-2 target gene encoding nucleocapsid 1 (N1)[7], while qPCR method B was based on the “LightMix® Modular Sarbecovirus E-gene” from TIB MOLBIOL (Berlin, Germany), distributed by Roche Diagnostics, and included primers to detect 76 bp fragments from the E gene from SARS and SARS-CoV-2 viruses[8].

In this study, we identified SARS-CoV-2 in a greater variety of tissues than those previously described[2,3,4]. Positive FFPE tissues using qPCR techniques included the oesophagus, large intestine, kidney, placenta, lung, and brain. Additionally, with IHC, we detected weak positivity in isolated cells in kidney, lung, brain, and histologically normal placentas. However, only one placenta sample showed strong diffuse IHC positivity.

SARS-CoV-2 RNA was previously detected in fresh gastrointestinal specimens obtained by endoscopy from oesophageal lesions and from stomach, duodenum and rectum samples in 3 of 6 patients, although no histopathological study was described[9]. The ACE2 receptor is highly expressed in oesophageal epithelial cells and absorptive enterocytes from the ileum and colon[10]. SARS-CoV-2 RNA was also previously detected in FFPE specimens from the oesophagus in autopsies, but it was not detected in the large intestine[11].

In postmortem FFPE core biopsies, Tian et al. detected SARS-CoV-2 RNA in the heart, lung, and liver[12]. In one autopsy, we were able to detect the virus in the lung and brain. Sekulic et al. (2020) found the highest SARS-CoV-2 RNA levels in FFPE tissues from the lung, bronchi, lymph nodes, and spleen in two limited autopsy cases (brain was not studied) using 2019-nCoV N1 and N2 primer/probe sets from IDT[11]. As in our autopsy case, in patients dying from diffuse alveolar damage, SARS-CoV-2 RNA may not be found in the kidney.

SARS-CoV-2 virus has also been successfully detected in FFPE tissue blocks from lung samples obtained in autopsies using a one-step RT–qPCR assay specific for the amplification of the SARS-CoV-2 E gene[13] or using immunofluorescence techniques with an antibody directed against the Rp3 NP protein[14].

In renal biopsies in COVID-19 patients, SARS-CoV-2 was detected using in situ hybridization in renal tubules and endothelial cells in six of nine (67%) kidney specimens, but IHC for SARS-CoV-2 spike protein was positive in only one case (11%)[15]. Using a primary antibody against the 2019-nCov N-protein, positive cases were found in 9/16 (56%) renal biopsies, with the virus mainly detected in proximal tubule epithelial cells and isolated distal tubule cells, with only one patient showing IHC positivity in more than 10% of the tubules. In this series, in situ hybridization was positive in 2/9 cases (22%), and real-time reverse-transcriptase polymerase chain reaction (RT–PCR) performed in FFPE tissue to detect the E and N1/N2 genes of SARS-CoV-2 in kidney samples was able to detect viral RNA in only 1/16 cases (6.25%)[16]. Most authors agree that SARS-CoV-2 can infect the kidney, at least in severe cases[17]. This confirms our findings suggesting that in COVID-19 patients, SARS-CoV-2 can occasionally be found in FFPE renal tissue using qPCR techniques, as in only one of 5 patients with a low viral load in our series, and IHC usually shows only a few positive epithelial tubular cells.

Most available studies have found that placentas from SARS-CoV-2-positive women do not show any specific histopathology pattern[18], although some authors have described a higher frequency of changes associated with maternal–foetal vascular malperfusion[19,20].

In our series, the highest SARS-CoV-2 virus load was detected in one placental FFPE specimen with inflammatory changes. With IHC, other authors confirmed the presence of the nucleocapsid protein of the virus in syncytiotrophoblasts, and no virus was identified in Hofbauer cells, but as in our series, isolated IHC-positive inflammatory cells for SARS-CoV-2 were also found in placental tissue[19,21,22]. In a series of 51 SARS-CoV-2-positive women, both IHC (using spike antibody) and in situ hybridization were negative in placental FFPE tissue[20].

We detected SARS-CoV-2 RNA using qPCR techniques in 3/5 placentas (60%). In a review of 19 studies that tested for SARS-CoV-2 RNA in the placenta, only 4 studies reported positive results[19]. Placental inflammatory changes in COVID-19 patients have been frequently described, but acute inflammatory changes are less frequent[19].

Positive cytology specimens in our series for qPCR included ascitic fluid, pleural fluid and urine. In ascitic fluid, the presence of SARS-CoV-2 RNA was first described by Culver et al. (2020) with a RT–PCR technique targeting the gene encoding the envelope (E) protein[23]. SARS-CoV-2 RT–PCR was also positive on nasopharyngeal swabs, bronchial aspirates and blood samples. Passarelli et al. (2020) also described SARS-CoV-2 RNA in ascitic fluid in a male patient with kidney transplantation, peritoneal dialysis, and liver cirrhosis, with ascitic fluid showing a significant number of macrophages[24]. Other authors were not able to detect SARS-CoV-2 in peritoneal or intra-abdominal samples in patients undergoing abdominal surgery[25].

SARS-CoV-2 has also been previously detected by RT–PCR in pleural fluid, showing reactive mesothelial cells and lymphocytes in cytology examination, in patients with lung infiltrates[26], and in children[27]. Viral RNA can also be detected in pleural fluid in patients without lung parenchyma involvement[28]. We detected SARS-CoV-2 RNA in one of the two pleural effusion samples examined in a patient with chronic heart failure, with no evidence of lung infiltrates.

Bennett et al. described a cytology of pleural fluid showing mesothelial cells with large multiple nuclei, consistent with the viral cytopathic effect in a COVID-19 patient[28]. We could not find any cytopathic effect of the virus in any of the tissue or cytology samples examined.

Urine samples have been reported to be positive for SARS-CoV-2 RNA in less than 1–19% of COVID-19 patients with a low or moderate viral load (approximately 300 copies/mL)[29,30]. We also detected SARS-CoV-2 RNA in urine using qPCR with the N1 target gene in a patient with persistent COVID-19 and a previous history of urothelial carcinoma, in which positive SARS-CoV-2 RNA in urine was detected long after RT–PCR from a nasopharyngeal swab became negative. A higher mortality rate has been described in patients with SARS-CoV-2 RNA positivity in urine[30]. Our patient was alive and well after 20 months of follow-up.

Liquid-based cytology has also been used for cytological and immunocytochemical studies of samples obtained with nasopharyngeal swabs. In this series, it was also confirmed that no viral cytopathic effect was found in epithelial cells, and granular cytoplasmic immunocytochemical positivity was observed only in nasopharyngeal squamous cells of SARS-CoV-2 RT–PCR-positive patients.

Macrophages and neutrophils did not show immunoreactivity. In this study, RT–PCR was not performed in liquid-based cytology medium[31].

In our series, the qPCR technique identified SARS-CoV-2 in specimens within an interval between nasopharyngeal PCR positivity and tissue/cytology sample collection ranging from 0 to 170 days. Considering the results of the two qPCR techniques, SARS-CoV-2 RNA could be identified in 25.58% of the selected tissue/cytology samples in COVID-19 patients.

Correlation analysis established that the shorter the interval and persistence time, the higher the viral load of the sample. This analysis is relevant to take into consideration, as samples obtained and submitted to different departments within short periods of time should be treated with additional precautions, since they will probably contain a high viral load.

We conclude that IHC cannot be used as a screening method, but it can offer useful data in patients with previous qPCR positivity in tissue or cytology. Strong IHC positivity in placental samples also showing acute villitis must be considered during histopathological examination of the placenta in COVID-19-positive women, especially when a lower Cp value (high viral load) is detected in qPCR techniques in placental FFPE tissue. In selected cases, both S and N protein antibodies can be reliably used in IHC to detect SARS-CoV-2[6].

We recommend the use of qPCR in FFPE tissue and liquid cytology samples, where SARS-CoV-2 RNA can also be detected. The selection of adequate nucleic acid extraction and qPCR techniques used can be very important to obtain reliable results. In these samples, we found higher sensitivity when using the automated nucleic acid extraction method from Qiagen and SARS-CoV-2 nucleocapsid 1 (N1) primers and probes from IDT technologies.

SARS-CoV-2 can be detected in multiple organs, and in some cases (e.g., lung or placenta), it may be associated with known histopathological findings, but we need larger cohorts to understand the long-term role of the presence of this virus in some organs.

Liquid cytology and FFPE tissue blocks are the most valuable sources of biological samples in scientific research, although even in well-processed specimens, RNA is increasingly degraded in FFPE archival samples with time[32]. However, with adequate methodology, SARS-CoV-2 can be detected in FFPE tissue blocks more than one year after sample collection.

Methods

Samples from patients

From an initial search in the electronic health record, 495 patients (18 years or older) in whom nasopharyngeal swabs were positive between March 2020 and February 2021 were retrospectively selected for a qPCR COVID-19 diagnostic test. Query terms employed for the electronic search included keywords such as “COVID-19”, “coronavirus” and “SARS-CoV-2”.

From these, we filtered 68 patients from whom a pathology specimen was also obtained and submitted to the Department of Pathology of the Hospital Universitario Puerta del Mar (HUPM) in Cadiz, Spain, as recorded in the Pathology Information System (VitroPath, Vitro SA, Seville, Spain).

The final sample size for this study consisted of 43 specimens with enough material to allow additional studies. These included cytology (liquid-based, and one cytology block obtained after fine-needle aspiration), autopsy, incisional biopsy (endoscopy, needle or Tru-Cut), and surgical or excisional specimens (including placentas).

All the samples and data were collected following the technical and ethical procedures of the local institutions and in accordance with the Helsinki Declaration. Informed consent was obtained from all subjects. The study was approved by the local Ethics Committee of the Province of Cadiz (96.20/129-N-20, approved on September 2020). The study was approved by the Andalusian Biomedical Research Ethics Committee, on the 30th of January 2018.

Interval, persistence and archival times

We defined interval as the time (in days) between the first positive qPCR result from a nasopharyngeal swab and the accession date of tissue or cytology specimen in the Department of Pathology. Negative interval values indicate that the patient tested positive for the

COVID-19 qPCR test from a nasopharyngeal swab after collection of the tissue or cytology specimen.

The time of persistence refers to the period (in days) between the first positive nasopharyngeal qPCR result and the subsequent first negative nasopharyngeal qPCR result. Archival time was defined as the period (in days) between specimen collection and RNA extraction.

Briefly, FFPE blocks were archived at room temperature (22 °C), and liquid-based cytology specimens were archived in a refrigerator (4 °C). Figure 3 shows a schematic representation of the interval, persistence and archival times.

Nucleic acid extraction and SARS-CoV-2 detection by qPCR

Two different qPCR techniques in tissue and cytology specimens were performed at the HUPM and the Pfizer Center (University of Granada-Junta de Andalusia) for Genomics and Oncology Research (GENYO), a reference centre in Andalusia, Spain, for molecular analysis of SARS-CoV-2.

In FFPE tissues (n=31), a common previous deparaffinization procedure was performed using 1 ml xylene and centrifuged at 10000 rpm for 2 minutes. The supernatant was discarded without disturbing the tissue pellet. The xylene step was repeated once more, followed by a 1 ml absolute 96-100% ethanol step. The tissue pellet was air dried, and 200 µl tissue lysis buffer provided in the kit and 20 µl proteinase K were added. The tissue was incubated at 56 °C until the tissue lysed completely. In liquid-based cytology samples (n=12), two previous centrifugation steps at 4.4 rpm for 5 minutes were performed.

qPCR method A (IDT Technologies)

All 43 samples were initially studied in GENYO. An RNeasy FFPE kit (Qiagen, Hilden, Germany) automated on QIAcube equipment was used for RNA isolation.

SARS-CoV-2 detection was performed using 7500 Real-Time PCR (Applied Biosystems™) equipment. TaqPath™ 1-Step RT–qPCR Master Mix (Applied Biosystems™) and a mix of primers and probes specific to the SARS-CoV-2 target gene N1 (IDT Technologies) were used following established protocols[7].

qPCR method B (Roche Diagnostics)

In 34 specimens where additional tissue or cytology was available, a second qPCR technique was performed in the Department of Pathology of HUPM. In these cases, a High Pure FFPET RNA Isolation kit (Roche Diagnostics, Indianapolis, IN) and Invitrogen™ Qubit™ 4 Fluorometer (Thermo Fisher Scientific, Whaltman, MD, USA) were used for RNA isolation and quantification, respectively.

For SARS-CoV-2 detection, a COBAS® z480 (Roche Diagnostics, Indianapolis, IN) analyser was used according to the protocol of the LightMix® Modular Sarbecovirus E-gene kit (Roche Diagnostics, Indianapolis, IN, USA)[8].

Detailed qPCR protocols are described in the Supplementary Material. In both qPCR methods, cycle threshold values less than 40 were considered positive.

Immunohistochemical study

IHC was performed in 29 FFPE samples. Each paraffin block was sectioned into two 3-µm-thick sections that were placed on Super Frost slides for standard IHC staining.

Two different primary antibodies were used. One of the slides was incubated with SARS-CoV Nucleoprotein/NP Antibody, Mouse Mab (Sino Biological, Catalogue number 40143-MM05), 1:300 dilution, for 32 minutes. A second slide was incubated with SARS-CoV Spike Antibody, Rabbit Pab (Sino Biological, Catalogue number 40150-T62-COV2), 1:100 dilution, for 32 minutes.

The immunohistochemistry technique was fully automated in a Roche Ventana BenchMark ULTRA IHC/ISH instrument.

(Ventana Medical Systems. Inc., Tucson, AZ, USA) using the DAB Optiview detection kit (Roche Diagnostics, Barcelona, Spain).

IHC slides were digitized using a PANNORAMIC® 250 Flash III DX scanner (3DHistech Ltd., Budapest, Hungary) with a resolution of 0.25 microns per pixel, obtaining digital slides in an MRXS file format. CaseViewer version 2.4.0.119028 was used to review digital slides.

Statistical analysis

First, a descriptive analysis was performed for quantitative and qualitative variables. Normality was assessed using the Kolmogorov–Smirnov and Shapiro–Wilk tests. For comparison between categorical variables, the $\chi 2$ test was used. Concordance between qPCR techniques was evaluated by the mean of Cohen´s Kappa index (κ).

The Spearman correlation test was used to compare the crossing points (Cp) obtained for positive qPCR and interval, persistence and archival times. The results are presented as the means ± standard deviation (SD) and 95% confidence intervals (CI).

All tests were two-sided, and statistical significance was defined as a p value below 0.05. IBM SPSS version 15.0 software (SPSS Inc., Chicago, IL, USA) was used to perform the statistical analysis.

Declarations

Acknowledgements

This work was supported by a grant (CV20-49543) from the General Secretary of Universities, Research and Technologies from the Andalusian Health System for research projects on SARS-CoV-2 (April 28th, 2020 Resolution), a postdoctoral grant (RH-0145-2020) from the Andalusia Health System, and the EU FEDER ITI Grant for Cadiz Province (PI-0032-2017).

We thank Esperanza de Santiago Rodríguez, PhD, and Luis Javier Martínez González, PhD, from the Genomic Unit of the Pfizer Center (University of Granada-Junta de Andalusia) for Genomics and Oncology Research (GENYO) for performing the molecular experiments for SARS-CoV-2 detection.

Availability of Data and Material

The datasets used and analysed in the current study available from the corresponding author on reasonable request.

Author contributions statement

I.B., A.S. and M.G. conceived the experiments; I.B. conducted the experiments; J.I., L.A., J.P., P.M., I.C., I.B., A.S. and M.G. analysed the results. All authors reviewed the manuscript.

Additional information

Competing interests: The authors declare that they have no conflicts of interest.

References

1. Zhu, N., Zhang, D., Wang, W., Li, X., Yang, B., Song, J., Zhao, X., Huang, B., Shi, W., Lu, R., Niu, P., Zhan, F., Ma, X., Wang, D., Xu, W., Wu, G., Gao, G. F., Tan, W. & China Novel Coronavirus Investigating and Research Team. A Novel Coronavirus from Patients with Pneumonia in China, 2019. *N. Engl. J. Med.* **382**(8), 727–733. https://doi.org/10.1056/NEJMoa2001017 (2020)
2. Barton, L. M., Duval, E. J., Stroberg, E., Ghosh, S. & Mukhopadhyay, S. COVID-19 Autopsies, Oklahoma, USA. *Am. J. Clin. Pathol.* **153**(6), 725–733. https://doi.org/10.1093/ajcp/aqaa062 (2020)

3. Menter, T., Haslbauer, J. D., Nienhold, R., Savic, S., Hopfer, H., Deigendesch, N., Frank, S., Turek, D., Willi, N., Pargger, H., Bassetti, S., Leuppi, J. D., Cathomas, G., Tolnay, M., Mertz, K. D. & Tzankov, A. Postmortem examination of COVID-19 patients reveals diffuse alveolar damage with severe capillary congestion and variegated findings in lungs and other organs suggesting vascular dysfunction. *Histopathology.* **77**(2), 198–209. https://doi.org/10.1111/his.14134 (2020)
4. Liu, J., Babka, A. M., Kearney, B. J., Radoshitzky, S. R., Kuhn, J. H. & Zeng, X. Molecular detection of SARS-CoV-2 in formalin-fixed, paraffin-embedded specimens. *JCI insight.* **5**(12), e139042. https://doi.org/10.1172/jci.insight.139042 (2020)
5. Zeng, Z., Xu, L., Xie, X. Y., Yan, H. L., Xie, B. J., Xu, W. Z., Liu, X. A., Kang, G. J., Jiang, W. L. & Yuan, J. P. Pulmonary pathology of early-phase COVID-19 pneumonia in a patient with a benign lung lesion. *Histopathology.* **77**(5), 823–831. https://doi.org/10.1111/his.14138 (2020)
6. Guerini-Rocco, E., Taormina, S. V., Vacirca, D., Ranghiero, A., Rappa, A., Fumagalli, C., Maffini, F., Rampinelli, C., Galetta, D., Tagliabue, M., Ansarin, M. & Barberis, M. SARS-CoV-2 detection in formalin-fixed paraffin-embedded tissue specimens from surgical resection of tongue squamous cell carcinoma. *J. Clin. Pathol.* **73**(11), 754–757. https://doi.org/10.1136/jclinpath-2020-206635 (2020)
7. https://eu.idtdna.com/pages/landing/coronavirus-research-reagents/cdc-assays
8. https://www.roche-as.es/lm_pdf/MDx_50-0776-96_Sarbecovirus-E-gene_RV_V200204_09164952001_CE-IVD.pdf
9. Lin, L., Jiang, X., Zhang, Z., Huang, S., Zhang, Z., Fang, Z., Gu, Z., Gao, L., Shi, H., Mai, L., Liu, Y., Lin, X., Lai, R., Yan, Z., Li, X. & Shan, H. Gastrointestinal symptoms of 95 cases with SARS-CoV-2 infection. *Gut.* **69**(6), 997–1001. https://doi.org/10.1136/gutjnl-2020-321013 (2020)
10. Tian, Y., Rong, L., Nian, W. & He, Y. Review article: gastrointestinal features in COVID-19 and the possibility of faecal transmission. *Aliment. Pharmacol. Ther.* **51**(9), 843–851. https://doi.org/10.1111/apt.15731 (2020)
11. Sekulic, M., Harper, H., Nezami, B. G., Shen, D. L., Sekulic, S. P., Koeth, A. T., Harding, C. V., Gilmore, H. & Sadri, N. Molecular Detection of SARS-CoV-2 Infection in FFPE Samples and Histopathologic Findings in Fatal SARS-CoV-2 Cases. *Am. J. Clin. Pathol.* **154**(2), 190–200. https://doi.org/10.1093/ajcp/aqaa091 (2020)
12. Tian, S., Xiong, Y., Liu, H., Niu, L., Guo, J., Liao, M. & Xiao, S. Y. Pathological study of the 2019 novel coronavirus disease (COVID-19) through postmortem core biopsies. *Mod. Pathol.* **33**(6), 1007–1014. https://doi.org/10.1038/s41379-020-0536-x (2020)
13. Van Campenhout, C., De Mendonça, R., Alexiou, B., De Clercq, S., Racu, M. L., Royer-Chardon, C., Rusu, S., Van Eycken, M., Artesi, M., Durkin, K., Mardulyn, P., Bours, V., Decaestecker, C., Remmelink, M., Salmon, I. & D'Haene, N. Severe Acute Respiratory Syndrome Coronavirus 2 (SARS-CoV-2) Genome Sequencing from Post-Mortem Formalin-Fixed, Paraffin-Embedded Lung Tissues. *J. Mol. Diag.* **23**(9), 1065–1077. https://doi.org/10.1016/j.jmoldx.2021.05.016 (2021)
14. Zhang, H., Zhou, P., Wei, Y., Yue, H., Wang, Y., Hu, M., Zhang, S., Cao, T., Yang, C., Li, M., Guo, G., Chen, X., Chen, Y., Lei, M., Liu, H., Zhao, J., Peng, P., Wang, C. Y. & Du, R. Histopathologic Changes and SARS-CoV-2 Immunostaining in the Lung of a Patient With COVID-19. *Ann. Intern. Med.* **172**(9), 629–632. https://doi.org/10.7326/M20-0533 (2020)
15. Pfister, F., Vonbrunn, E., Ries, T., Jäck, H. M., Überla, K., Lochnit, G., Sheriff, A., Herrmann, M., Büttner-Herold, M., Amann, K. & Daniel, C. Complement Activation in Kidneys of Patients With COVID-19. *Front. Immunol.* **11**, 594849. https://doi.org/10.3389/fimmu.2020.594849 (2021)
16. Bouquegneau, A., Stéphanie Grosch, E., Habran, L., Hougrand, O., Huart, J., Krzesinski, JM., Misset, B., Hayette, MP., Delvenne, P., Bovy, C., Kylies, D., Huber, TB., Puelles, VG., Delanaye, P. & Jouret, F. (2021) COVID-19–associated Nephropathy Includes Tubular Necrosis and Capillary Congestion, with Evidence of SARS-CoV-2 in the Nephron. *Kidney360.* **2**(4) 639-652. https://doi.org/10.34067/KID.000699202 (2021)
17. Khan, S., Chen, L., Yang, C. R., Raghuram, V., Khundmiri, S. J. & Knepper, M. A. Does SARS-CoV-2 Infect the Kidney? *J. Am. Soc. Nephrol.* **1**(12), 2746–2748. https://doi.org/10.1681/ASN.2020081229 (2020)
18. He, M., Skaria, P., Kreutz, K., Chen, L., Hagemann, I. S., Carter, E. B., Mysorekar, I. U., Nelson, D. M., Pfeifer, J. & Dehner, L. P. (2020). Histopathology of Third Trimester Placenta from SARS-CoV-2-Positive Women. *Fetal and pediatric pathology.* 1–10. Advance online publication. https://doi.org/10.1080/15513815.2020.1828517
19. Sharps, M. C., Hayes, D., Lee, S., Zou, Z., Brady, C. A., Almoghrabi, Y., Kerby, A., Tamber, K. K., Jones, C. J., Adams Waldorf, K. M. & Heazell, A. A structured review of placental morphology and histopathological lesions associated with SARS-CoV-2 infection. *Placenta.* **101**, 13–29. https://doi.org/10.1016/j.placenta.2020.08.018 (2020)
20. Smithgall, M. C., Liu-Jarin, X., Hamele-Bena, D., Cimic, A., Mourad, M., Debelenko, L. & Chen, X. Third-trimester placentas of severe acute respiratory syndrome coronavirus 2 (SARS-CoV-2)-positive women: histomorphology, including viral immunohistochemistry and in-situ hybridization. *Histopathology.* **77**(6), 994–999. https://doi.org/10.1111/his.14215 (2020)

21. Hecht, J. L., Quade, B., Deshpande, V., Mino-Kenudson, M., Ting, D. T., Desai, N., Dygulska, B., Heyman, T., Salafia, C., Shen, D., Bates, S. V. & Roberts, D. J. SARS-CoV-2 can infect the placenta and is not associated with specific placental histopathology: a series of 19 placentas from COVID-19-positive mothers. *Mod. Pathol.* **33**(11), 2092–2103. https://doi.org/10.1038/s41379-020-0639-4 (2020)
22. Morotti, D., Cadamuro, M., Rigoli, E., Sonzogni, A., Gianatti, A., Parolin, C., Patanè, L. & Schwartz, D. A. Molecular Pathology Analysis of SARS-CoV-2 in Syncytiotrophoblast and Hofbauer Cells in Placenta from a Pregnant Woman and Fetus with COVID-19. *Pathogens.* **10**(4), 479. https://doi.org/10.3390/pathogens10040479 (2021)
23. Culver, A., Arbelot, C., Bechis, C., Cassir, N. & Leone, M. First description of SARS-CoV-2 in ascites. *IDCases.* 21, e00836. https://doi.org/10.1016/j.idcr.2020.e00836 (2020)
24. Passarelli, V. C., Perosa, A. H., de Souza Luna, L. K., Conte, D. D., Nascimento, O. A., Ota-Arakaki, J. & Bellei, N. Detected SARS-CoV-2 in Ascitic Fluid Followed by Cryptococcemia: a Case Report. *SN. Compr. Clin. Med.* https://doi.org/10.1007/s42399-020-00574-9 (2020)
25. Romero-Velez, G., Rodriguez Quintero, J. H., Pereira, X., Nussbaum, J. E. & McAuliffe, J. C. SARS-CoV-2 During Abdominal Operations: Are Surgeons at Risk? *Surg. Laparosc. Endosc. Percutan. Tech.* **31**(6), 674–678. https://doi.org/10.1097/SLE.0000000000000971 (2021)
26. Mei, F., Bonifazi, M., Menzo, S., Di Marco Berardino, A., Sediari, M., Paolini, L., Re, A., Gonnelli, F., Duranti, C., Grilli, M., Vennarucci, G. S., Latini, M. A., Zuccatosta, L. & Gasparini, S. First Detection of SARS-CoV-2 by Real-Time Reverse Transcriptase-Polymerase Chain Reaction Assay in Pleural Fluid. *Chest.* **158**(4), e143–e146. https://doi.org/10.1016/j.chest.2020.05.583 (2020)
27. Yousefzadegan, S., Mahmoudabadi, R. Z. & Gharehbaghi, G. A 6-Year-Old Boy with COVID-19-Positive Pleural Effusion and Kawasaki-Like Features. *Case Rep. Pediatr.* 8832826. https://doi.org/10.1155/2021/8832826 (2021)
28. Bennett, D., Franchi, F., De Vita, E., Mazzei, M. A., Volterrani, L., Disanto, M. G., Garosi, G., Guarnieri, A., Cusi, M. G., Bargagli, E., Scolletta, S., Valente, S., Gusinu, R. & Frediani, B. SARS-CoV-2 in pleural fluid in a kidney transplant patient. *Postgrad. Med.* **133**(5), 540–543. https://doi.org/10.1080/00325481.2020.1838817 (2021)
29. Peng, L., Liu, J., Xu, W., Luo, Q., Chen, D., Lei, Z., Huang, Z., Li, X., Deng, K., Lin, B. & Gao, Z. (2020). SARS-CoV-2 can be detected in urine, blood, anal swabs, and oropharyngeal swabs specimens. *J. Med. Virol.* **92**(9), 1676–1680. https://doi.org/10.1002/jmv.25936 (2020)
30. Marand, A., Bach, C., Janssen, D., Heesakkers, J., Ghojazadeh, M., Vögeli, T. A., Salehi-Pourmehr, H., Mostafae, H., Hajebrahimi, S. & Rahnama'i, M. S. Lower urinary tract signs and symptoms in patients with COVID-19. *BMC Infect. Dis.* **21**(1), 706. https://doi.org/10.1186/s12879-021-06394-z (2021)
31. Parada, D., Peña, K. B., Gumà, J., Guilarte, C. & Riu, F. Liquid-based cytological and immunohistochemical study of nasopharyngeal swab from persons under investigation for SARS-CoV-2 infection. *Histopathology.* **78**(4), 586–592. https://doi.org/10.1111/his.14257 (2021)
32. Sánchez-Navarro, I., Gámez-Pozo, A., González-Barón, M., Pinto-Marín, A., Hardisson, D., López, R., Madero, R., Cejas, P., Mendiola, M., Espinosa, E. & Vara, J. A. Comparison of gene expression profiling by reverse transcription quantitative PCR between fresh frozen and formalin-fixed, paraffin-embedded breast cancer tissues. *BioTechniques.* **48**(5), 389–397. https://doi.org/10.2144/000113388 (2010)

Figures

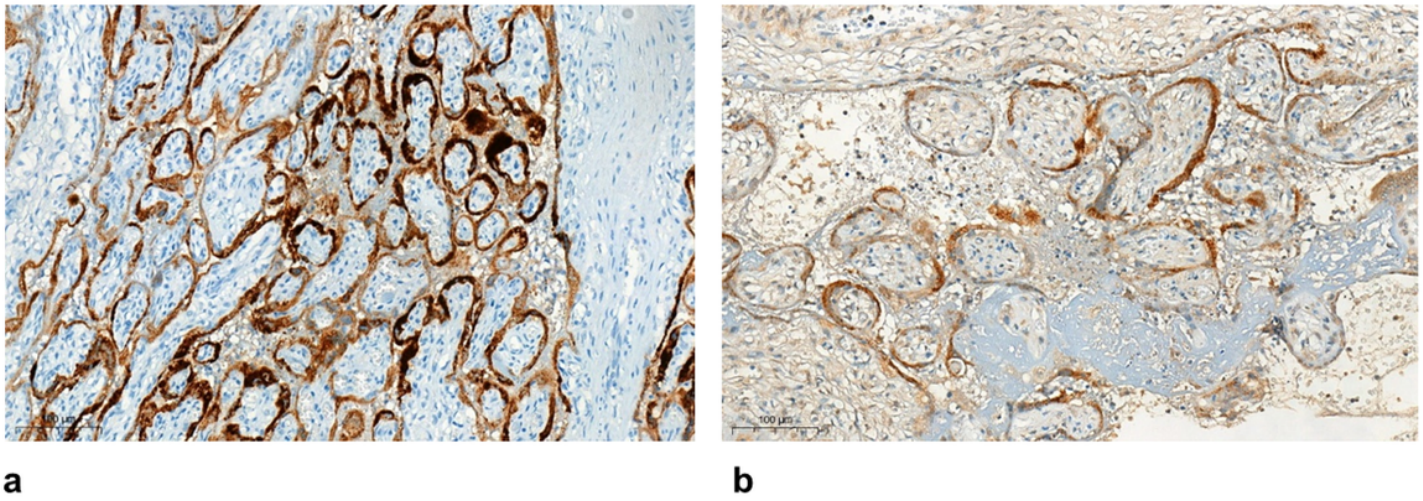

Figure 1

Strong diffuse immunohistochemical positivity for both the nucleoprotein (a) and spike (b) protein of SARS-CoV-2 in a syncytiotrophoblast specimen (case 22) (magnification 20x).

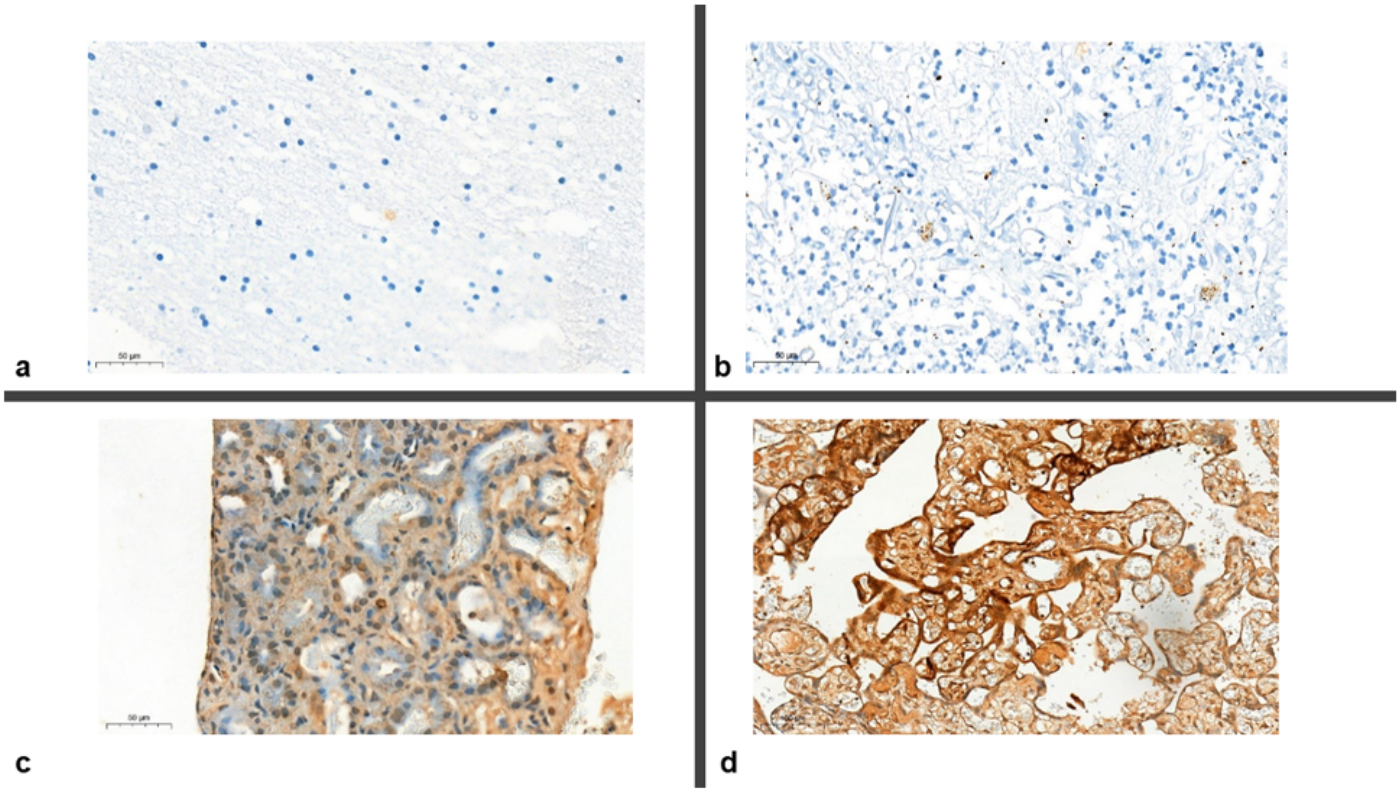

Figure 2

Weakly isolated immunohistochemical positivity for the nucleoprotein in the lung and brain (a, b) and for the spike protein of SARS-CoV-2 in the kidney and placenta (c, d) (magnification 40x).

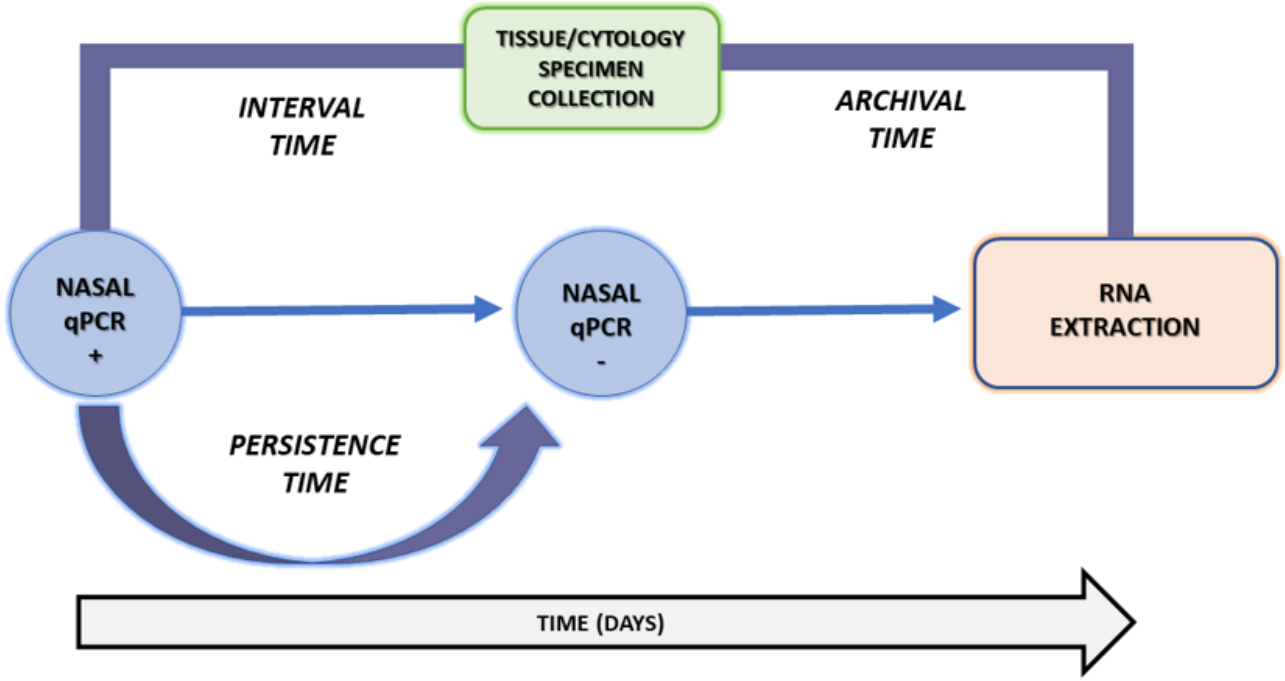

Figure 3

Schematic representation of interval, persistence and archival times

Supplementary Files

This is a list of supplementary files associated with this preprint. Click to download.

- SupplementarymaterialSARSCoV2.pdf